Conjunctival vaccination against *Brucella ovis* in mice with mannosylated nanoparticles

Raquel Da Costa Martins[1], Carlos Gamazo[2], María Sánchez-Martínez[3], Montserrat Barberán[4], Ivan Peñuelas[3], Juan M. Irache[1]

[1]Dpt. Pharmacy and Pharmaceutical Technology, University of Navarra, Pamplona, Spain
[2]Dpt. Microbiology, University of Navarra, Pamplona, Spain
[3]Radiopharmacy Unit. Department of Nuclear Medicine, University Clinic of Navarra, Pamplona, 31008, Spain
[4]Dpt. of Animal Pathology, University of Zaragoza, Zaragoza, Spain

Corresponding author
Juan M. Irache
Farmacia y Tecnología Farmacéutica
University of Navarra
C/Irunlarrea, 1
31080 – Pamplona
Spain
e-mail: jmirache@unav.es
Phone: +34 948425600

Graphical abstract

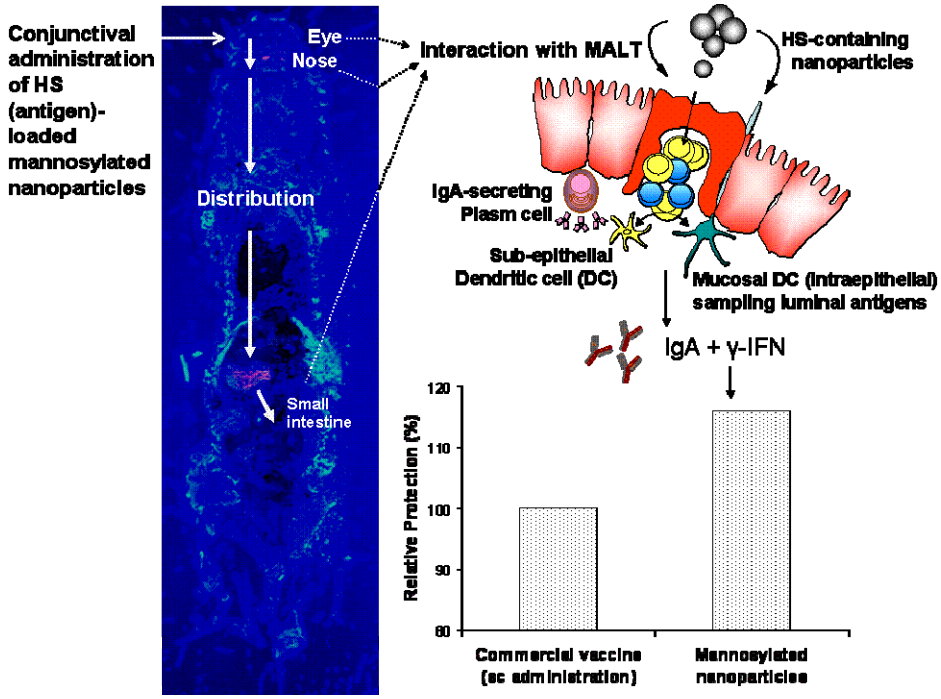

Abstract
The use of sub-unit vaccines can solve some drawbacks associated with traditional attenuated or inactivated ones. However, in order to improve their immunogenicity, these vaccines needs to be associated to an appropriate adjuvant which, adequately selected, may also offer an alternative pathway for administration. The aim of this work was to evaluate the protection offered by the hot saline complex extracted from *Brucella ovis* (HS) encapsulated in mannosylated nanoparticles (MAN-NP-HS) when instilled conjunctivally in mice. Nanoparticles displayed a size of 300 nm and the antigen loading was close to 30 µg per mg nanoparticle. Importantly, encapsulated HS maintained its protein profile, structural integrity and antigenicity during and after the preparative process of nanoparticles. The ocular immunization was performed on BALB/c mice. Eight weeks after vaccination animals were challenged with *B. ovis*, and 3 weeks later, were slaughtered for bacteriological examinations. Animals immunized with MAN-NP-HS displayed a 3-log reduction in spleen CFU compared with unvaccinated animals. This degree of protection was significantly higher than that observed for the commercial vaccine (Rev1) subcutaneously administered. Interestingly, the mucosal IgA response induced by MAN-NP-HS was found to be much more intense that that offered by Rev1 and prolonged in time. Furthermore, the elicited IL-2, IL-4 and γ-IFN levels showed good correlation with the degree of protection. On the other hand, biodistribution studies in animals were performed with nanoparticles labelled with either ^{99m}technetium or rhodamine B isothiocyanate. The biodistribution revealed that, after instillation, MAN-NP-HS moved from the palpebral area to the nasal region and, the gastrointestinal tract. This profile of distribution was different to that observed for free $^{99m}TcO_4^-$ colloids, which remained for at least 24 hours in the site of administration. In summary, mannosylated nanoparticles appear to be a safe and suitable adjuvant for conjunctival vaccination.

Keywords: Brucellosis; Nanoparticles; Vaccine; Mannose; Mucosal immunization; Biodistribution.

List of abbreviations
^{99m}Tc: ^{99m}technetium
$^{99m}TcO_4^-$: ^{99m}technetium pertechnetate
APCs: antigen presenting cells
BALT: bronchial-associated lymphoid tissue
BSS: buffered saline solution
CALT: conjunctiva-associated lymphoid tissue
CFU: colony forming units
DMF: dimethylformamide
EE: entrapment efficiency
H&E: haematoxylin-eosin stain
HS: hot saline subcellular complex extracted from *Brucella ovis*
GALT: gut-associated lymphoid tissue
MALT: mucosa-associated lymphoid tissue
MAN-NP: mannosylated poly(anhydride) nanoparticles
MAN-NP-HS: HS-loaded mannosylated poly(anhydride) nanoparticles
NALT: nasal-associated lymphoid tissue
PBS-T: solution of Tween 20 (0.05% w/v) in PBS
RBITC: rhodamine B isothiocyanate
SALT: skin-associated lymphoid tissue

1. Introduction

Brucellosis is a zoonotic infection transmitted from animals to humans by direct- or indirect contact with infected animals or their products such as the ingestion of raw milk and other unpasteurized dairy products (i.e. soft cheeses) [1, 2]. Other common routes of infection in humans include infection through cuts and abrasions, the conjunctival sac of the eyes or the inhalation of aerosols [3, 4]. In livestock, the main route of infection is via the sucking or licking of aborted foetuses and their placentas, as well as vaginal discharges. Infection due to the ingestion of infected milk or feedstuffs may also occur [1]. Human brucellosis remains the commonest zoonotic disease worldwide with more than 500,000 new cases annually [5]. Furthermore this infection is associated with substantial residual disability, and is an important cause of travel-associated morbidity [6].

Mass vaccination of animal populations accompanied by a strict surveillance scheme is a first step to reduce the number of infected animals and hence the infection pressure in regions where the incidence rate of animal brucellosis is high. The most commonly used vaccines are *Brucella melitensis* Rev1 and *Brucella abortus* S19 vaccines [7]. *B. abortus* RB51 vaccine is also used in some countries [8].

The *B. melitensis* Rev1 strain is currently considered as the best vaccine available for the control of ovine and caprine brucellosis, especially when used at the standard dose by either the subcutaneous or the conjunctival routes [9, 10]. However, due to its live attenuated nature, Rev1 displays a large number of drawbacks, including residual virulence and interferences with serodiagnosis [8]. In order to solve some of these drawbacks, the use of sub-unit vaccines have been proposed such as the hot saline subcellular complex extracted from *B. ovis* (HS) [11]. However, due to its non-replicant nature, adequate adjuvants have to be associated. In this context, poly(ε-caprolactone) microparticles containing HS were found to be safe and effective in mice and ram models, when administered by the subcutaneous route [12, 13]. However, regarding the behaviour of *Brucella* during the infection and colonization processes, the delivery of the antigens (HS) through mucosal surfaces is of remarkable interest in order to both mimic the bacteria pattern and generate immunity at the major portals of entry for these microorganisms.

Mucosal surfaces, mostly the subepithelial regions, are enriched in immunocompetent B and T lymphocytes, as well as antigen presenting cells (APCs). These cells are organized into the mucosa-associated lymphoid tissue (MALT) found in various sites of the body such as the gut (GALT), lung (BALT) or skin (SALT), among others [14]. In the eye, the conjunctiva, the palpebral area and the eye lachrymal drainage system are provided with an associated lymphoid tissue (termed CALT, conjunctiva-associated lymphoid tissue) [15] containing the specialized antigen sampling M-cells [16] present at other mucosal localizations, such as intestinal Peyer's patches. Furthermore, evidences from many studies have confirmed the inter-connected mucosal system, known as common mucosa immune system, allowing that the stimulation at one mucosal site can lead to effector immune cells in local as well as distal mucosal surfaces [14]. In addition to these immunological reasons, mucosa vaccination can also be safer and easier to dispense than traditional (parenteral) vaccines [17, 18].

In the last years, nanoparticles made from the copolymer of methyl vinyl ether and maleic anhydride (Gantrez® AN) have demonstrated a remarkable capability to induce immune responses when administered orally [19-21]. This last property can be potentiated and modulated by the "decoration" of the surface of these poly(anhydride) nanoparticles with ligands capable to recognize and bind to specific

components of the MALT. Among other ligands, mannose and its derivatives may be of interest due to the capability of these compounds to link with mannose receptors highly expressed in cells of the mucosal immune system (i.e. macrophages and dendritic cells) [22, 23].
The aim of this work was to evaluate the protection offered by the HS-loaded mannosylated poly(anhydride) nanoparticles, when administered conjunctivally as eye drops, against experimental *B. ovis* infection in mice. Moreover, the biodistribution of these nanoparticles after their administration was evaluated.

2. Material and Methods

2.1. Chemicals

Poly(methyl vinyl ether-co-maleic anhydride) or poly(anhydride) [Gantrez® AN 119; Mw 200 KDa] was gifted by ISP (Spain). Mannosamine hydrochloride, rhodamine B isothiocyanate (RBITC), concanavalin A and Tween 20 were purchased from Sigma-Aldrich (Spain). Antibodies peroxidase/ conjugate anti-IgA were supplied from Nordic Immunol. Labs (The Netherlands). BCA™ Protein Assay Reagent Kit was from Pierce (USA). Acrylamide Criterion XT Precast gels (18 Comb, 30 µL, 1 mm) were obtained from Bio-Rad Laboratories (USA). PVDF (pore size of 0.45 µm) sheets were from Schleicher & Schuell (Germany) and 4-chloro 1-naphtol from Merck (Germany). Blood Agar Base plates were from BioMérieux SA (France) and O.C.T.™ was obtained from Sakura (The Netherlands). RPMI 1640 media, β-mercaptoethanol, penicillin, streptomycin, FBS, sterile PBS and sodium pyruvate were purchased from Gibco-BRL (UK). ^{99}Mo-^{99m}Tc generator was from Drytec (GE Healthcare, UK). Acetone, ethanol and dimethyl formamide (DMF) were obtained from BDH-Prolabo/VWR (France). Stannous chloride, methylethylketone and potassium perchlorate, were from Panreac (Spain). T-61 was from Intevet (Spain) and the isoflurane (Isoflo™) from Esteve (UK). All other chemicals used were of analytical grade and obtained from Fluka (Spain).

2.2. Extraction and characterization of the hot saline antigenic complex (HS)

The hot saline antigenic complex (HS) was obtained from the strain *B. ovis* REO 198 incubated in a bioreactor as described previously [24]. Total protein and lipopolysaccharide content of each batch of the antigenic extract were determined by the BCA™ Protein Assay and the Warren modified method [24], respectively. The HS used to prepare the nanoparticles contained 66.4±10.6% total proteins and 39.5±3.8% rough lipopolysaccharide.

2.3. Preparation and labeling of nanoparticles

2.3.1. Preparation of HS-loaded mannosylated nanoparticles

Poly(anhydride) HS-loaded mannosylated nanoparticles (MAN-NP-HS) were prepared by the solvent displacement method as described previously [20, 25]. Briefly, four mg of the HS antigenic extract were dispersed in acetone an added to 100 mg of Gantrez® AN 119 dissolved in acetone, previously incubated overnight with 1 mg of mannosamine. After 30 min of incubation, nanoparticles were formed by the addition of an ethanol/water mixture (1:1 v/v). Once the organic solvents were eliminated under reduced pressure (Büchi R-144, Switzerland), the aqueous nanosuspensions were magnetically stirred for 1 h with mannosamine. The resulting nanoparticles were purified twice at 3,000 x g for 20 min by centrifugal filtration in tubes VivaSpin® 20 300,000 MWCO (Vivascience, Germany). Filtrates were

collected for the quantification of HS and mannosamine. Finally, formulations were freeze-dried with sucrose at 5% as cryoprotector (Genesis 12EL, Virtis, USA).
Control mannosylated nanoparticles (MAN-NP) were prepared using the same methodology without the use of HS.

2.3.2. HS-loaded mannosylated nanoparticles labeled with RBITC

HS-loaded nanoparticles were fluorescently labeled by incubation with 1.25 mg of rhodamine B isothiocyanate (RBITC) for 5 min at room temperature [20, 25]. After adsorption of the marker, the nanoparticles were purified by centrifugation and, finally, freeze-dried as described above.

2.3.3. HS-loaded mannosylated nanoparticles labeled with ^{99m}Tc

Nanoparticles were radiolabeled with ^{99m}Tc by reduction of ^{99m}Tc-Pertecnetate ($^{99m}TcO_4^-$) with stannous chloride as described previously [26]. Briefly, 20 µL of a stannous chloride solution were added to 1 mg of freeze-dried nanoparticles followed by addition of 74 MBq of freshly eluted $^{99m}TcO_4^-$ in 0.5 mL. The mixture was vortexed for 30 seconds and incubated at room temperature for 10 min. The pH of the final suspension was adjusted to 4.

2.4. Characterization of nanoparticles

2.4.1. Size, zeta potential, morphology and yield

The size and zeta potential of the nanoparticles were determined by photon correlation spectroscopy and electrophoretic laser Doppler anemometry, respectively, using a Zetamaster analyser system (Malvern Instruments, UK). The yield of the nanoparticles preparation process was determined by gravimetry from freeze-dried nanoparticles as described previously [20].
The morphological characteristics of the nanoparticles were observed by electron microscopy in a Zeiss DSM 940A microscope (Oberkochen, Germany) coupled with a digital image system (Point Electronic GmBh, Germany). Previously, nanoparticles were diluted with deionised water and centrifuged at 17,000 rpm (Sigma 3K30, Germany) for 20 min. The pellet was dried and shaded with a 9 nm gold layer in a Emitech K 550 Sputter-Coater (Ashford, UK).

2.4.2. Quantification of HS loaded in nanoparticles

The HS loading in the nanoparticles was quantified by the BCA™ Protein Assay method from the difference between its initial concentration added and the concentration found in the collected filtrates obtained during purification. Each sample was assayed in triplicate. To evaluate the effect of the manufacturing process on the HS protein integrity profile and antigenicity, proteins from the freeze-dried nanoparticles were extracted with a mixture of acetone and DMF (3:1, v/v) and assayed by SDS-PAGE and immunoblotting using sera from naturally infected rams with *B. ovis* [24].

2.4.3. Mannosamine content and agglutination assay

The amount of mannosamine associated to nanoparticles was estimated by difference between the initial amount added and the amount quantified in the supernatants collected during the purification step of the preparative process [20]. In order to verify the activity of the mannosamine associated to the surface of nanoparticles an *in vitro* agglutination assay was performed. For this purpose mannosamine nanoparticles were dispersed in water and incubated with

concanavalin A. The turbidity changes were measured in a spectrophotometer at 405 nm, as described previously [20].

2.5. Protective effect of HS-loaded mannosylated nanoparticles

Animal experiments were performed according to the policies and guidelines of the responsible Committee of the University of Navarra in line with the European legislation on animal experiments (86/609/EU) and following a protocol approved by the Ethic Committee of the University of Navarra.

2.5.1. Ocular immunization and challenge with *B. ovis*

The protective efficacy of HS-loaded nanoparticles against the virulent *B. ovis* PA strain was conducted in BALB/c mice, using the *B. melitensis* Rev1 vaccine as a reference. Twenty four female BALB/c mice (8 weeks old supplied by Harlan, Spain), were placed into rack conditions and divided in four groups. Animals were conjunctivally immunized with 8 µL of one of the following treatments administered in each eye: (i) 12 µg HS-loaded in mannosylated nanoparticles (MAN-NP-HS), (ii) empty nanoparticles (MAN-NP) equivalent to the dose administered in the first group, and (iii) sterile Buffered Saline Solution (BSS) as unvaccinated control group. As reference, Rev1 was subcutaneously administered once ($5x10^5$ CFU/mouse in 100 µL BSS). Faecal IgA, antibodies against HS and γ-IFN, IL-2 and IL-4 cytokines (from spleen and lymph node cells) were determined.

Eight weeks after vaccination, mice were challenged intraperitoneally with $5\ x10^4$ CFU/mouse of the virulent *B. ovis* PA reference strain. Three weeks after infection, animals were sacrificed by cervical dislocation, and the spleens were aseptically removed. Then, samples were individually homogenized in BSS, and properly diluted and plated in Blood Agar Base for viable counts. Plates were incubated for 3-5 days at 37±1 ºC in a 10% CO_2 atmosphere. The protection level conferred by each preparation was expressed as the mean ± SD (n=6) of the CFU of the virulent challenge strain per spleen, after logarithmic conversion.

2.5.2. Faecal specific IgA anti-HS

Faecal samples from each group of mice were collected into microtubes and weighed. Non-fatty milk in PBS (3%) was added at a ratio of 1 mL/100 mg faecal pellets, vortexed for 5 min at room temperature and centrifuged at 10,000 x g for 10 min. Supernatants were transferred to tubes containing 10 µL of protease inhibitor and stored at -20°C until use. Analysis of faecal samples was conducted as described elsewhere [29]. Briefly, HS-coated plates were blocked with 200 µL of 3% non-fatty milk in PBS-0.05% Tween 20 (PBS-T) for 1 h, at room temperature. Faecal extract samples of 100 µL diluted 1:2 in PBS-T were added and incubated at 37 ºC for 4 h. Finally, washed wells were treated with antibodies peroxidase/conjugated anti-IgA in a 1:1000 dilution. The detection was carried out with H_2O_2-ABTS and the absorbance was determined at λ_{max} 405 nm.

2.5.3. Cytokine assay

Immunized animals were sacrificed 4 or 8 weeks after administration to remove spleens and lymph nodes (axillary, brachial, cervical and mesenteric). Isolated cells obtained as described previously [12] were stimulated with HS (100 µg) and cultured at 37ºC with 12% CO_2 during 48 h for IL-2 and IL-4, and during 72 h for γ-IFN quantification. Released cytokines were determined with the correspondent commercial sandwich ELISA kit (Biosource™, USA).

2.5.4. Anatomopathological studies

Accordingly to OECD 405 guidelines for the testing of chemicals (*in vivo* test for acute eye irritation/corrosion) [27], during the days following the instillation of nanoparticles, all the animals were inspected for local reactions. In addition, 1-day and 3-days after immunization, female BALB/c mice (n = 4) were sacrificed. Eye samples were fixed in 10% buffered formalin, embedded in paraffin and 4-5 µm sections were stained with haematoxylin-eosin (H&E stain) using standard procedures for microscopic examination.

2.6. Biodistribution of nanoparticles

The studies were performed after approval by the responsible Ethical Committee of the University of Navarra in strict accordance with the European legislation in animal experiments.

2.6.1. Studies with fluorescently labeled nanoparticles

A single dose of RBITC-labeled MAN-NP-HS containing 12 µg of HS in 8 µL water for injection was conjunctivally administrated in each eye of BALB/c mice. The animals were sacrificed 4 h later and the eyes, nose and portions from the gastrointestinal tract of about 0.5 cm length were removed and washed with PBS. Then, samples were treated with O.C.T.™, frozen in liquid nitrogen and stored at -20 ºC. Tissue samples were cut into 5 µm longitudinal sections in a cryostat (2800 Frigocut E, Reichert-Jung, Germany), attached to glass slides and visualized by fluorescence microscopy (Olympus U-RFLT50, Japan).

Additionally, two animals received one conjunctival dose per eye of 8 µL RBITC-labeled MAN-NP-HS containing 12 µg of HS, and 4 h post-administration were euthanized with T-61 (after anaesthesia with 2% isoflurane), frozen in liquid nitrogen, treated with O.C.T.™ and stored at -20 ºC. Entire animals were then cut into 40 µm longitudinal sections in a cryostat (2800 Frigocut E, Reichert-Jung, Germany), attached to tap slides, and visualized with a fluorescence source and photographed (Olympus U-RFLT50, Japan).

2.6.2. Studies with radiolabelled nanoparticles

One hour before the ocular administration of HS-loaded nanoparticles as eye drops, animals were treated by the intravenous route with a solution of potassium perchlorate in saline (3 mg/kg). Then, animals received a single ocular dose of 8 µL containing ^{99m}Tc-MAN-NP-HS nanoparticles (2.37 MBq, 12 µg HS per eye) and were divided in two groups. The first group of animals was euthanized with T-61, at 4 h post-administration (as indicated above) frozen in liquid nitrogen, treated with O.C.T.™ and stored at -20 ºC. Entire animals were then sliced into 20 µm longitudinal sections in a cryostat (Bright 8250, Bright Instrument Co Ltd, UK), and exposed to digital autoradiography imaging plates (BAS-SR 2025, Fujifilm, Japan) for 20 min. Then, the images were read in a digital autoradiography instrument and treated with the Raytest BAS500 reader 3.14 software (Fujifilm, Japan). The second group of animals was euthanized either 2- or 24-h after the administration of radiolabeled nanoparticles. Then, lymph nodes, stomach, small intestine, large intestine, spleen, liver, kidney, palpebral area, eyes and nose were collected, weighed, and the radioactivity of each organ was measured in a gamma counter (1282 Compugamma CS, LKB Pharmacia, Finland) calibrated for ^{99m}Tc energy. Results were expressed as counts per minute per gram of each organ divided by the

total counts per the total weight of the whole organs [(cpm/organ weight)/(total cpm/total weight]. In these studies a control group of animals receiving the equivalent dose of free technetium was used.

2.7. Statistical analysis

Data were expressed as the mean ± S.D. of at least three experiments. Statistical significance analysis was carried out using the non-parametric Kruskal-Wallis test, followed by Mann-Whitney *U*-test. *P* values of < 0.05 were considered as statistically significant. Calculations were performed using SPSS 16.0.1 software (USA).

3. Results

3.1. Physicochemical characterization of nanoparticles

Table 1 summarizes the main physicochemical properties of nanoparticles used in this study. Mannosylated nanoparticles displayed a mean size of about 270 nm whereas the encapsulation of HS yielded higher nanoparticles (about 300 nm). The morphological analysis by scanning electron microscopy confirmed the presence of spherical particles with a similar size to that obtained by photon correlation spectroscopy (Figure 1). The presence of HS did not really affect the negative zeta potential of nanoparticles. Similarly, the yield of the preparative process and the homogeneity of the different batches prepared (polydispersity of about 0.2 ± 0.1) was found to be similar for both control and HS-loaded nanoparticles.

The mannosamine content was found to be about 30 µg mannosamine per mg of nanoparticles. The agglutination test in the presence of the mannose-specific Concanavalin A confirmed the mannose integrity and activity after mannosylation of poly(anhydride) nanoparticles (data not shown). HS loading was calculated to be 28 µg HS per mg of nanoparticles with an encapsulation efficiency close to 70%. The integrity and antigenicity of HS after its encapsulation in nanoparticles was evaluated, after extraction from the carriers, by SDS-PAGE and Western blot. In both cases, the protein profile of HS extracted from nanoparticles was similar to free HS, and the immunobloting demonstrated a similar reactivity against a pool of sera from *B. ovis* experimentally infected rabbits, showing that the antigenicity of the main proteins involved in infection was conserved (data not shown).

Table 1. Physico-chemical characteristics of nanoparticles. MAN-NP: empty mannosylated poly(anhydride) nanoparticles; MAN-NP-HS: HS-loaded nanoparticles. Data expressed as mean ±SD, n=10.

Formulation	Size (nm)	Zeta potential (mV)	Yield (%)	Man conten (µg/mg NP)	HS loading (µg/mg NP)	EE (%)
MAN-NP	272±12	-38.2±1.4	81±6	30.2±4.1	-	-
MAN-NP-HS	306±11	-34.6±1.3	80±5	32.1±4.7	28.3±1.9	69±1

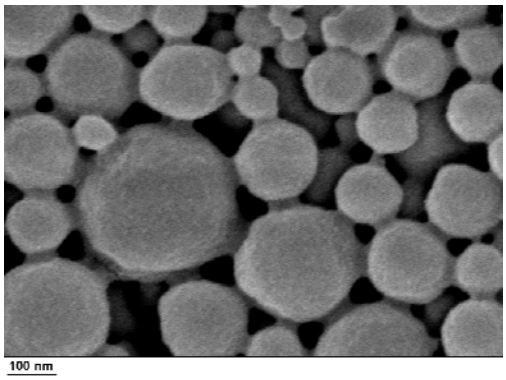

Figure 1. Scanning electron microscopy (SEM) microphotographs from a lyophilized sample of MAN-NP-HS.

3.2. Mice immunization studies

Figure 2 shows the levels of specific IgA against HS elicited at 4- and 8- weeks after immunization. The mucosal IgA response after immunization with HS-mannosylated nanoparticles was found to be intense and prolonged in time. Thus, 8-weeks post-immunization, the faecal IgA elicited response was found to be 2-times higher for MAN-NP-HS than for Rev1.

Figure 3 shows the levels of cytokines at 4- and 8- weeks after immunization with MAN-NP, MAN-NP-HS or Rev1, secreted from spleen cells or lymph nodes after in vitro stimulation with HS. MAN-NP-HS and Rev1 elicited similar responses and they showed significant differences from unvaccinated animals ($p < 0.05$) especially for γ-IFN. Differences were higher with the spleen cells at the 8th week. In contrast, the highest values of cytokines secreted by cells from lymph nodes were obtained 4 weeks post-administration.

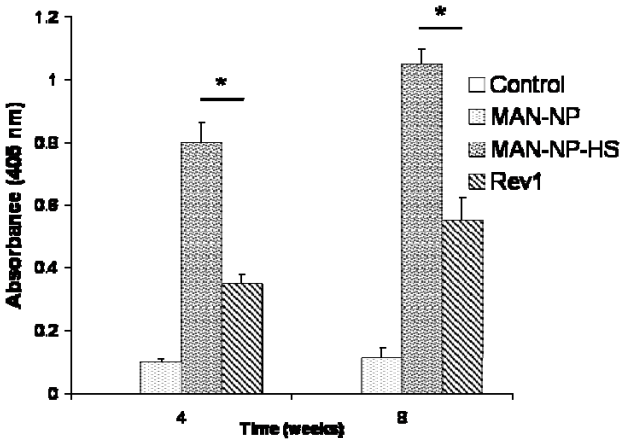

Figure 2. Faecal anti-IgA elicited by BALB/c mice after subcutaneous immunization with *B. melitensis* Rev1 or ocular immunization with empty mannosylated nanoparticles (MAN-NP) and HS-loaded mannosylated nanoparticles (MAN-NP-HS). Control: animals treated with BSS. * $p < 0.01$, Mann-Whitney *U*-test.

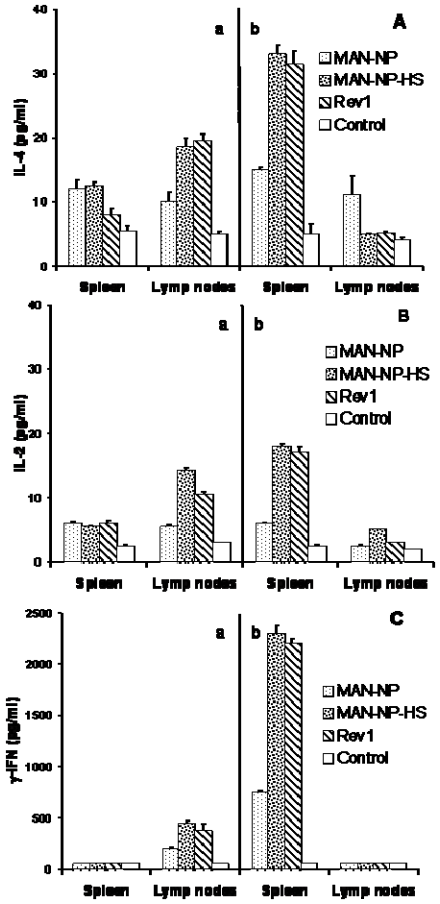

Figure 3. Cytokines secretion from spleen and lymph node cells after HS stimulus, elicited in BALB/c mice after immunization with *B. melitensis* Rev1 vaccine (Rev1), mannosylated nanoparticles (MAN-NP) or HS-loaded mannosylated nanoparticles (MAN-NP-HS). A: levels of IL-4; B: levels of IL-2; C: levels of gamma-interpheron. Data refers to values quantified 4 weeks (a) or 8 weeks (b) post-immunization.

3.3. Protection studies

Table 2 summarizes the bacteriological results obtained after challenge of the immunized mice with *B. ovis* PA strain. Mannosylated nanoparticles loaded with HS and conjunctivally administered as eye drops offered the highest degree of protection with respect unvaccinated control group (3.7 vs 6.6 Log CFU/spleen), even higher than that offered by the Rev1 vaccination by the subcutaneous route ($p < 0.01$).

Table 2. Protective efficacy of HS-loaded mannosylated nanoparticles (MAN-NP-HS), conjunctivally administered, after challenge with the virulent *Brucella ovis* PA strain. MAN-NP: empty mannosylated nanoparticles, Rev1: *B. melitensis* Rev1 vaccine sc administered. Data expressed as mean and SD (n=6) of log CFU of *B. ovis* per spleen for each group of vaccinated and unvaccinated mice (control group).

Immunization strategy	Mean±SD Log (CFU/spleen)	Statistical differences vs[1]			
		MAN-NP	MAN-NP HS	Rev1	Control (BSS)
MAN-NP	4.62±0.27	-	A	A	A
MAN-NP HS	3.69±0.13	-	-	A	A
Rev1	4.10±0.22	-	-	-	A

Control (BSS)	6.62±0.21	-	-	-	-

[1] Statistical differences between the immunized groups (non-parametric by Mann-Whitney *U*-test): A: $p < 0.01$ regarding the CFU/spleen of the animals

3.4. Pathological studies

After conjunctival immunization, animals were inspected for irritation symptom or lesions due to the instillation and presence of nanoparticles in the eyes. Macroscopically, neither ulceration nor opacity was observed in the cornea. Furthermore, the iris presented an apparently normal aspect with absence of chemosis. However, during the first 24 h after the administration of nanoparticles, some eyes displayed hyperaemic blood vessels and redness. In any case, since the animals did not develop apparent ocular damage, the study ended 3 days post instillation.

Figure 4 shows microphotographs from the eyes of animals after the instillation of mannosylated nanoparticles. Compared with samples from animals treated with water for injections and which presented normal aspects (data not shown), eyes treated with nanoparticles displayed some inflammatory cells in the periphery of lymphoid follicles (CALT) and in the nictitating membrane (Figure 3A). In addition, some inflammatory cells, mainly neutrophils, could be observed into capillaries and perivascular tissue in the ciliary body of the eyes three days after immunization (Figure 3B and 3C).

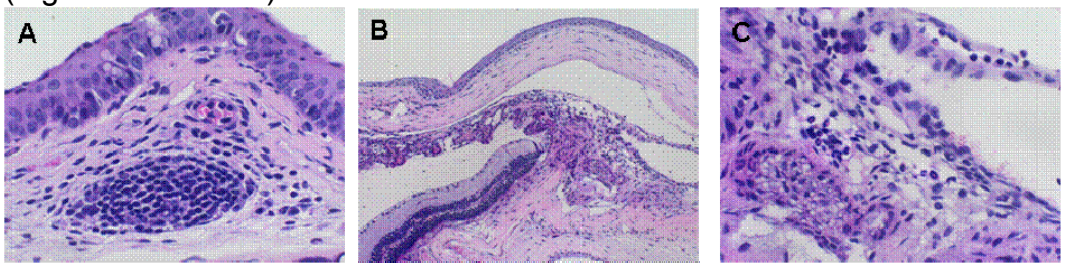

Figure 4. Histologic tissue sections of eyes from mice, 1 day (A) and 3 days (B and C) after instillation of mannosylated nanoparticles. A: presence of moderate numbers of lymphocytes and plasma cells at the periphery of a lymphoid follicle in the nictitating membrane CALT, (H&E stain, 400x) B: Mild inflammatory reaction of ciliary body (H&E stain, 100x); C: Detail of figure B showing neutrophils as the main component of the inflammatory infiltrate (H&E stain, 400x).

3.5. Biodistribution studies of nanoparticles after ocular administration of fluorescent and radiolabeled nanoparticles

In order to study the distribution of MAN-NP-HS after administration as eye drops, the nanoparticles were labeled with either RBITC or ^{99m}Tc. Figure 5A shows the distribution of RBITC in the body and in different organs of the animals 4 h after the ocular administration of a single dose of fluorescently labeled nanoparticles. RBITC was visualized in the eyes, nasal duct, stomach and intestine. From a microscopic study, it was possible to corroborate the presence of the fluorescent marker in the site of administration (cornea, conjunctive and lachrymal sac), but also at the nasal associated lymphoid tissue (NALT) and Peyer's patches of the ileum of animals (Figure 6).

This pattern of distribution was confirmed by autoradiography after radiolabeling of HS loaded mannosylated nanoparticles with ^{99m}Tc (Figure 5B). In this case, intense radioactivity was found in the ocular mucosa as well as in the gastrointestinal tract.

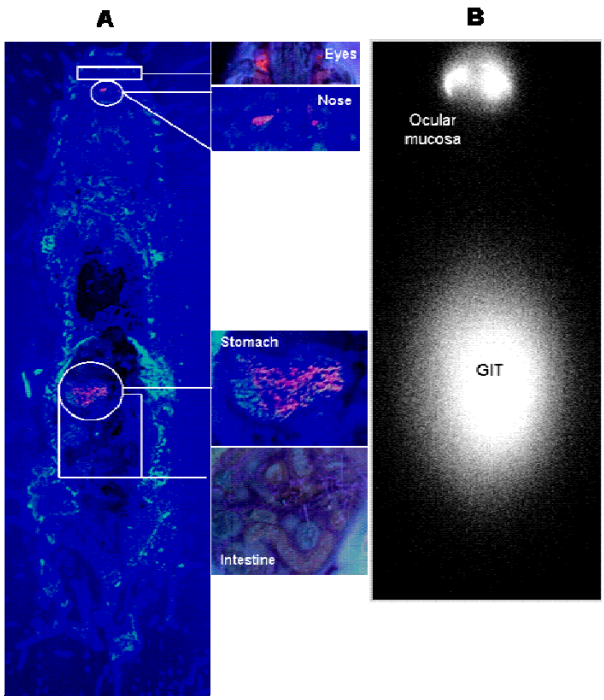

Figure 5. Fate of nanoparticles (MAN-NP-HS) fluorescently labeled with RBITC (A) or radiomarked with ^{99m}Tc (B), 4-h after their administration by instillation in the eyes of animals. Fluorescence is visualized in the eyes, nose, stomach and intestines of the animal (A). Mice autoradiograph shows radioactivity in the site of administration and the gastrointestinal tract (B).

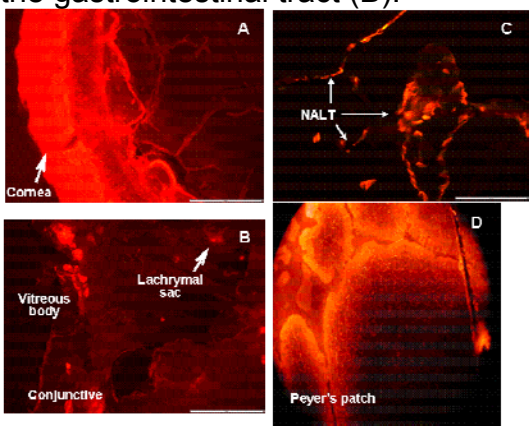

Figure 6. Visualization of RBITC, in different organs of the animals, 4-h after the instillation of MAN-NP-HS fluorescently labeled. (A) Cornea (magnification 100x); (B) Eye of animals (magnification 100x); (C) Nose sample (magnification 400x); (D) Intestinal Peyer patch (magnification of 400x).

In order to confirm these results, *ex vivo* biodistribution studies were conducted. Radiolabeled nanoparticles were conjunctivally administered and animals were sacrificed either 2 or 24 h post administration. The different organs were recovered for measuring the radioactivity in a gamma-counter. Figure 7 summarizes these results. When free $^{99m}TcO_4^-$ instead of ^{99m}Tc-radiolabeld nanoparticles was administered, radioactivity (around 80%) was mainly found in the palpebral area (lids). On the contrary, radiolabeled nanoparticles dramatically modified the biodistribution of the radioactive marker, and significant levels of radioactivity were found in the stomach, intestines, eyes and nose. Another important fact was that the

amount of radioactivity found in the animal's stomach decreased with time, whereas it increased in the large intestine.

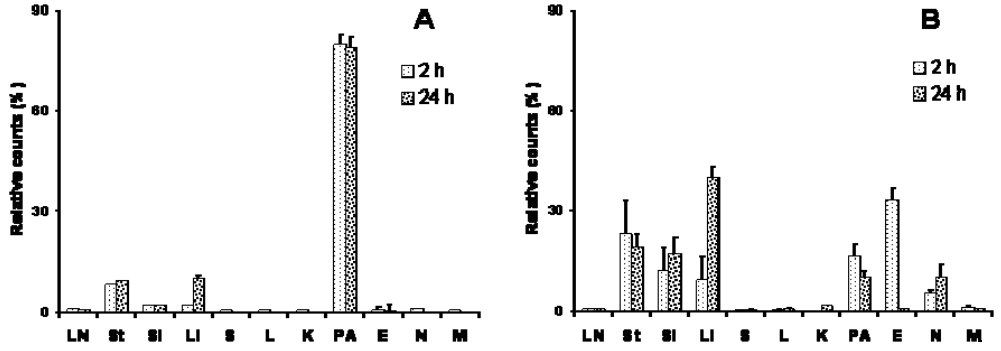

Figure 7. Biodistribution studies of free $^{99m}TcO_4^-$ (A) and ^{99m}Tc-labeled MAN-NP-HS (B). Animals were sacrificed either 2 or 24 hours post-conjunctival administration. The radioactivity of each organ was expressed as counts per minute per gram of each organ divided by the total counts per the total weight of the whole organs. Each value represents the mean ± SD of 3 animals. Legend: LN: lymph nodes; St: stomach; SI: small intestine; LI: large intestine; S: spleen; L: liver; K: kidney; PA: palpebral area (lids) and CALT; E: eye; N: nose and NALT; M: mouth.

4. Discussion

It is well known that the ocular bioavailability of drugs applied topically as eye-drops is typically poor. The absorption of drugs in the eye is limited by some protective mechanisms (i.e. lachrymation and tear turnover; drainage via the conjunctival sac) and other factors such as the limited corneal area and poor permeability. The drainage of the administered dose via the nasolachrymal system takes place when the volume of fluid in the eye exceeds the normal lachrymal volume. More important, the lachrymation and the physiological tear turnover are stimulated by the instillation of even mildly irritating fluids compromising bioavailability [28, 29]. Under these circumstances it appears that the induction of immune responses through instillation of a vaccine in the eye would be an important challenge.

In this context, the aim of this work was to evaluate the protective effect of a new conjunctival vaccine against brucellosis based on the loading of the *B. ovis* HS antigenic complex in mannosylated poly(anhydride) nanoparticles. Mannosylation of nanoparticles was carried out in order to target mannose receptors, which are highly expressed in cells of the immune system (i.e. macrophages and dendritic cells) [30] and are involved in antigen capture and presentation [31]. The HS-loaded nanoparticles were obtained as a dry powder which was put easily in suspension by the addition of water. The dispersed nanoparticles displayed a size of about 300 nm with an antigen loading of about 30 µg HS per mg nanoparticle (Table 1). These nanoparticles displayed a relatively smooth surface (Figure 1).

After the conjunctival administration of HS-loaded mannosylated nanoparticles high levels of specific mucosal IgA were detected (Figure 2). At the same time, this nanoparticle formulation induced high and similar levels of Th1 (γ-IFN and IL2) and Th2 (IL4) cytokines than the commercial Rev1 vaccine (Figure 3). Specifically, γ-IFN has been defined as a key actor in the cellular immune response necessary to eliminate intracellular bacteria, like *Brucella* [32, 33]. Thus, both effector components, mucosal anti-*Brucella* IgA and Th1 immunity would be directly related with the level

of protection conferred by MAN-NP-HS, even higher than that conferred by the Rev1 vaccine (Table 2) [34, 35].
Interestingly, the conjunctival administration of MAN-NP-HS in mice did not induce significant levels of inflammatory cells post-immunization (Figure 4). With the exception of mild inflammatory perivascular infiltrates localized in the ciliary body of a mouse inoculated with nanoparticles, animals did not develop microscopic lesions in the eyes. All the components of the anterior chamber, cornea, iris, pupil, and the lens, optic nerve, nictitating membranes and bulbar conjunctiva lacked injuries and had a histologic normal appearance. This almost complete absence of injuries in all the ocular structures proves that instillations of mannosylated nanoparticles by ocular way in mouse are not-irritating to eyes and satisfy the OECD 405 guidelines for the testing of chemicals [27].
The biodistribution study clearly shown that, after the instillation of nanoparticles in the eye, a fraction of these carriers remained in the site of administration whereas a significant percentage of the dose migrated to other areas of the body such as the nose mucosa and the gastrointestinal tract. Within the gut, labeled nanoparticles were mainly detected in the stomach and the intestine, including Peyer's patches (see Figures 5 and 6). On the other hand, the distribution of free ^{99m}Tc-pertechnetate and ^{99m}Tc-radiolabeled nanoparticles was completely different. Free technetium was mainly detected in the palpebral area (lids), with slight detection in the stomach or other parts of the body (Figure 7).
Interestingly, the profile of biodistribution of nanoparticles was independent of the type of labeling used, either fluorescent (rhodamine B isothyocyanate) or radioactive (^{99m}Tc). In fact, this distribution agrees well with the physiological mechanisms of clearance which protects the surface of the eye. In fact, the excess of liquid in contact with the surface of the eye, due to the lid movement, is drained through the conjunctival sac, the lachrymal sac and into the nasolachrymal duct into the nose. Then, from the nose, the liquids can easily reach the gastrointestinal tract [36].
This profile of distribution of nanoparticles, when administered topically as eye drops, may be responsible for their ability to induce protective immune response. In fact, one portal of entry would permit to reach at least three different mucosal surfaces and, thus, induce simultaneous response against the pathogen in different effector sites of the body.

5. Conclusions

In summary, HS-loaded in mannosylated nanoparticles appears to be an interesting vaccine candidate when conjunctivally administered as eye drops. This efficacy would be related with their distribution after instillation. In fact, the excess of nanoparticle suspension, via the lachrymal drainage system, is capable to reach the nose and the gastrointestinal tract. In all of these mucosa nanoparticles can encounter APCs and, thus, induce and potentiate the immune response.

Acknowledgements

This work was supported by "Fundação para a Ciência e Tecnologia" (SFRH/BD/41703/2007) in Portugal, "Asociación de Amigos de la Universidad de Navarra", "Fundación Caja Navarra" ("Nanotecnología y Medicamentos", ref. 10828), and grants from the Ministerio Ciencia e Innovación (AGL2004-07088, PPT-420000-2008-4) and "Ministerio Sanidad y Consumo (IF0663617-2) in Spain.

References

[1] M.J. Corbel, Brucellosis: an overview, Emerg. Infect. Dis. 3 (1997) 213–222.
[2] S.D. Thakur, R. Kumar, D.C. Thapliyal, Human brucellosis: review of an under-diagnosed animal transmitted disease, J. Commun. Dis. 34 (2002) 287-301.
[3] G. Pappas, N. Akritidis, M. Bosilkovski, E. Tsianos, Brucellosis, N. Engl. J. Med. 352 (2005) 2325–2336.
[4] I. Rolando, L. Olarte, G. Vilchez, M. Lluncor, L. Otero, M. Paris, C. Carrillo, E. Gotuzzo, Ocular manifestations associated with brucellosis: a 26-year experience in Peru, Clin. Infect. Dis. 46 (2008) 1338-1345.
[5] G. Pappas, P. Papadimitriou, N. Akritidis, L. Christou, E.V. Tsianos, The new global map of human brucellosis. Lancet Infect. Dis. 6 (2006) 91-99.
[6] Z.A. Memish, H.H. Balkhy, Brucellosis and international travel, J. Travel. Med. 11 (2004) 49–55.
[7] H. Smits, M. Kadri, Brucellosis in India: a deceptive infectious disease, Indian J. Med. Res. 122 (2005) 375-384.
[8] R. Adone, M. Francia, F. Ciuchini, Evaluation of *Brucella melitensis* B115 as rough phenotype vaccine against *B. melitensis* and *B. ovis* infection, Vaccine 26 (2008) 4913-4917.
[9] J.M. Blasco, A review of the use of *B. melitensis* Rev 1 vaccine in adult sheep and goats, Prev. Vet. Med. 31(1997) 275-283.
[10] B. Garin-Bastuji, J.M. Blasco, M. Grayon, J.M. Verger, *Brucella melitensis* infection in sheep: present and future, Vet. Res. 29 (1998) 255-274.
[11] C. Gamazo, A.J. Winter, I. Moriyon, J.I. Riezu-Boj, J.M. Blasco, R. Diaz, Comparative analyses of proteins extracted by hot saline or released spontaneously into outer membrane blebs from field strains of *Brucella ovis* and *Brucella melitensis*, Infect. Immun. 57 (1989) 1419-1426.
[12] M. Murillo, M.J. Grillo, J. Rene, C.M. Marin, M. Barberan, M.M. Goni, J.M. Blasco, J.M. Irache, C. Gamazo, A *Brucella ovis* antigenic complex bearing poly-epsilon-caprolactone microparticles confer protection against experimental brucellosis in mice, Vaccine 19 (2001) 4099-4106.
[13] R. Da Costa Martins, J.M. Irache, J.M. Blasco, M.P. Munoz, C.M. Marin, M.J. Grillo, M.J. De Miguel, M. Barberán, C. Gamazo, Evaluation of particulate acellular vaccines against *Brucella ovis* infection in rams, Vaccine 28 (2010) 3038-3046.
[14] B. Pulendran, R. Ahmed, Immunological mechanisms of vaccination, Nat. Immunol. 12 (2011) 509–517(2011).
[15] C.K. Petris, M. Golomb, T.E. Philipps, Bacterial transcytosis across conjunctival Mcells,. Invest. Ophthalmol. Vis. Sci. 48 (2007) 2172-2177.
[16] H. Liu, C.K. Meagher, C.P. Moore, T.E. Phillips, Mcells in the follicle-associated epithelium of the rabbit conjunctiva preferentially binds and translocate latex beads, Invest. Ophthalmol. Vis. Sci. 46 (2005) 4217-4223.
[17] G. Dietrich, M. Griot-Wenk, I.C. Metcalfe, A.B. Lang, J.F. Viret, Experience with registered mucosal vaccines, Vaccine 21 (2003) 678-683.
[18] S. Chadwick, C. Kriegel, M. Amiji, Nanotechnology solutions for mucosal immunization, Adv. Drug Deliv. Rev. 62 (2010) 394-407.
[19] M. Estevan, J.M. Irache, M.J. Grillo, J.M. Blasco, C. Gamazo, Encapsulation of antigenic extracts of *Salmonella enterica* serovar *abortusovis* into polymeric systems and efficacy as vaccines in mice, Vet. Microbiol. 118 (2006) 124-132.
[20] H.H. Salman, C. Gamazo, M.A. Campanero, J.M. Irache, Bioadhesive mannosylated nanoparticles for oral drug delivery, J. Nanosci. Nanotechnol. 6 (2006) 3203-3209.

[21] H.H. Salman, C. Gamazo, P.C. de Smidt, G. Russell-Jones, J.M. Irache, Evaluation of bioadhesive capacity and immunoadjuvant properties of vitamin B(12)-Gantrez nanoparticles, Pharm. Res. 25 (2008) 2859-2868.
[22] B. Carrillo-Conde, E.H. Song, A. Chavez-Santoscoy, Y. Phanse, A.E. Ramer-Tait, N.L. Pohl, M.J. Wannemuehler, B.H. Bellaire, B. Narasimhan, Mannose-functionalized "pathogen-like" polyanhydride nanoparticles target C-type lectin receptors on dendritic cells, Mol. Pharm. 8 (2011) 1877-1886.
[23] A.M. Kerrigan, G.D. Brown, C-type lectins and phagocytosis, Immunobiology 214 (2009) 562-575.
[24] R. Da Costa Martins, C. Gamazo, J.M. Irache, Design and influence of g-irradiation on the biopharmaceutical properties of nanoparticles containing an antigenic complex from *Brucella ovis*, Eur. J. Pharm. Sci. 37 (2009) 563–572.
[25] P. Arbos, M. Wirth, M.A. Arangoa, F. Gabor, J.M. Irache, Gantrez AN as a new polymer for the preparation of ligand-nanoparticle conjugates, J Control Release 83 (2002) 321-330.
[26] P. Areses, M. Agueros, G. Quincoces, M. Collantes, J.A. Richter, L.M. Lopez-Sanchez, M. Sánchez-Martínez, J.M. Irache, I. Peñuelas, Molecular imaging techniques to study the biodistribution of orally administered (99m)Tc-labelled naive and ligand-tagged nanoparticles, Mol. Imaging Biol. 13 (2011) 1215-1223.
[27] Organization for Economic Cooperation and Development, Test No. 405. Acute eye irritation/corrosion,. OECD Guidelines for the Testing of Chemicals, Section 4, OECD Publishing, (2002) doi: 10.1787/9789264070646-en
[28] R.D. Schoenwald, S. Vidvauns, D.E. Wurster, C.F. Barfknecht, Tear film stability of protein extracts from dry eye patients administered a sigma agonist, J. Ocul. Pharmacol. Ther. 13 (1997) 151-161.
[29] N. Yokoi, A.J. Bron, J.M. Tiffany, K. Maruyama, A. Komuro, S. Kinoshita, Relationship between tear volume and tear meniscus curvature, Arch. Ophtalmol. 122 (2004) 1265-1269.
[30] T. Keler, V. Ramakrishna, M.W. Fanger, Mannose receptor-targeted vaccines. Expert Opin. Biol. Ther. 4 (2004) 1953-1962.
[31] K. Gijzen, A. Cambi, R. Torensma, C.G. Figdor, C-type lectins on dendritic cells and their interaction with pathogen-derived and endogenous glycoconjugates, Curr. Protein Pept. Sci. 7 (2006) 283-294.
[32] E.A. Murphy, J. Sathiyaseelan, M.A. Parent, B. Zou, C.L. Baldwin, Interferon-γ is crucial for surviving a *Brucella abortus* infection in both resistant C57BL/6 and susceptible BALB/c mice, Immunol. 103 (2001) 511–518.
[33] P. Skendros, G. Pappas, P. Boura, Cell-mediated immunity in human brucellosis, Microbes. Infect. 13 (2011) 134-142.
[34] M.V. Delpino, S.M. Estein, C.A. Fossati, P.C. Baldi, Nonpathogenic alphaproteobacteria in mice by immunization with partial protection against *Brucella* infection, Clin. Vaccine Immunol. 14 (2007) 1296-1301.
[35] V. Suraud, M. Olivier, C.C. Bodier, L.A. Guilloteau, Differential expression of homing receptors and vascular addressins in tonsils and draining lymph nodes: effect of *Brucella* infection in sheep, Vet. Immunol. Immunopathol. 15 (2007) 239-250.
[36] V. Singh, R. Ahmad, T. Heming, The challenges of ophthalmic drug delivery: a review, Int. J. Drug Discover. 3 (2011) 56-62